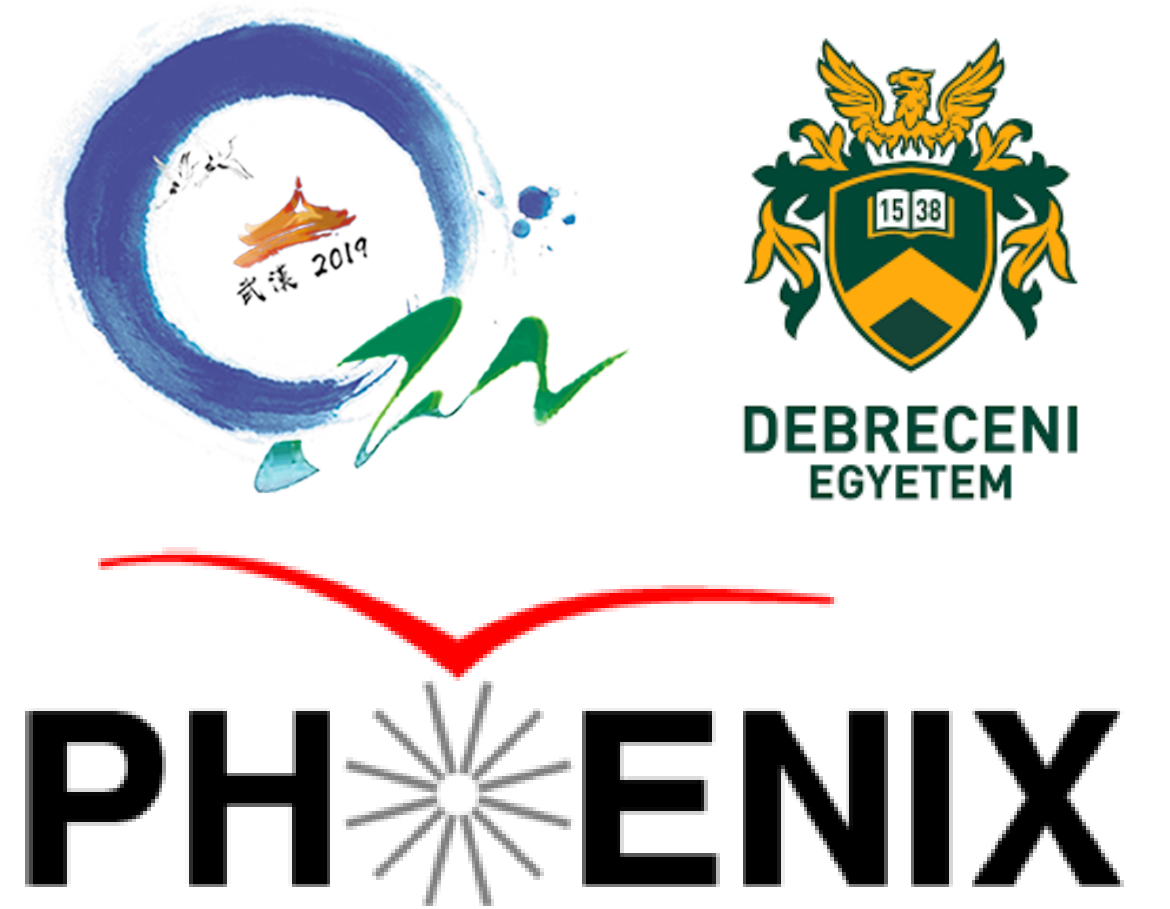


# High transverse momentum direct photons in p+Au collisions in PHENIX at RHIC

Zhandong Sun for the PHENIX collaboration

University of Debrecen, Hungary

sunzdchina@gmail.com



## Introduction

High transverse momentum ( $p_T$ ) direct photons are penetrating probes in relativistic heavy ion collisions: once produced, they leave the collision region virtually unaffected, even if a hot, dense partonic medium was formed. This is also the reason why direct photons are immune to the suppression observed for high  $p_T$  hadrons and jets in heavy ion collisions. The nuclear modification factor of high  $p_T$  photons is unity in Au+Au collisions if the p+p yields are scaled by the number of nucleon-nucleon collisions calculated from the Glauber-model [1]. We assume that high transverse momentum direct photons are a "standard candle" for initial hard scattering, and, per extension, for collision geometry not only for p+p and A+A, but also for small-on-large collisions. If true, comparing the centrality dependence of direct photon and hadron production in p+Au is a robust test of the applicability of the Glauber model in such systems. The first measurement of high  $p_T$  photons in asymmetric collisions (d+Au) is shown in Fig. 1.

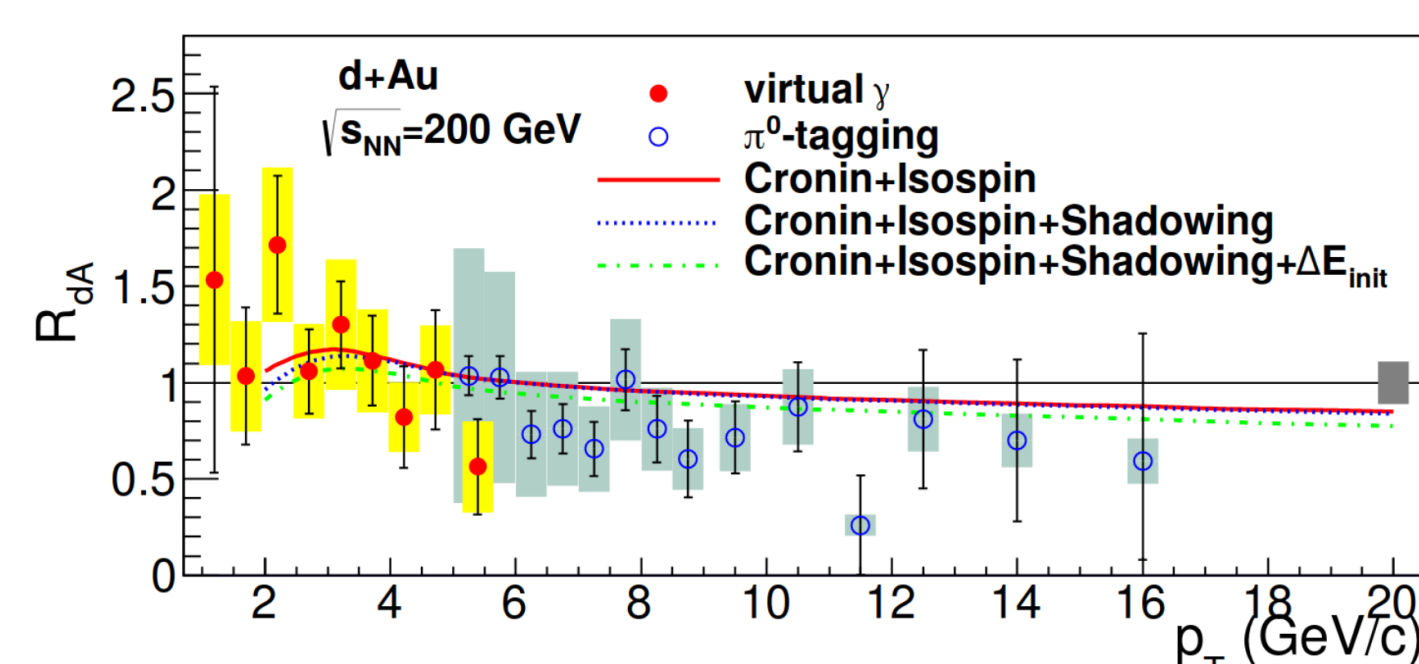


**Figure 1:** Nuclear modification factor for photons in d+Au collisions ( $R_{dA}$ ), as a function of  $p_T$ . The closed and open symbols show the results from the virtual- and real-photon measurements, respectively. Figure taken from [2].

In this poster we report on the status of the analysis of high transverse momentum direct photons in p+Au collisions at various centralities as well as of the direct photon / hadron ratios and its comparison with hadron production. The main detector used is the Electromagnetic Calorimeter (EMCal). The data of minimum bias (BBC) and triggered (ERT) p+Au collisions in PHENIX from the 2015 data taking period (Run 15) are used in this study. The expected significance of the measurement based solely on statistical uncertainties is shown in Fig. 2.

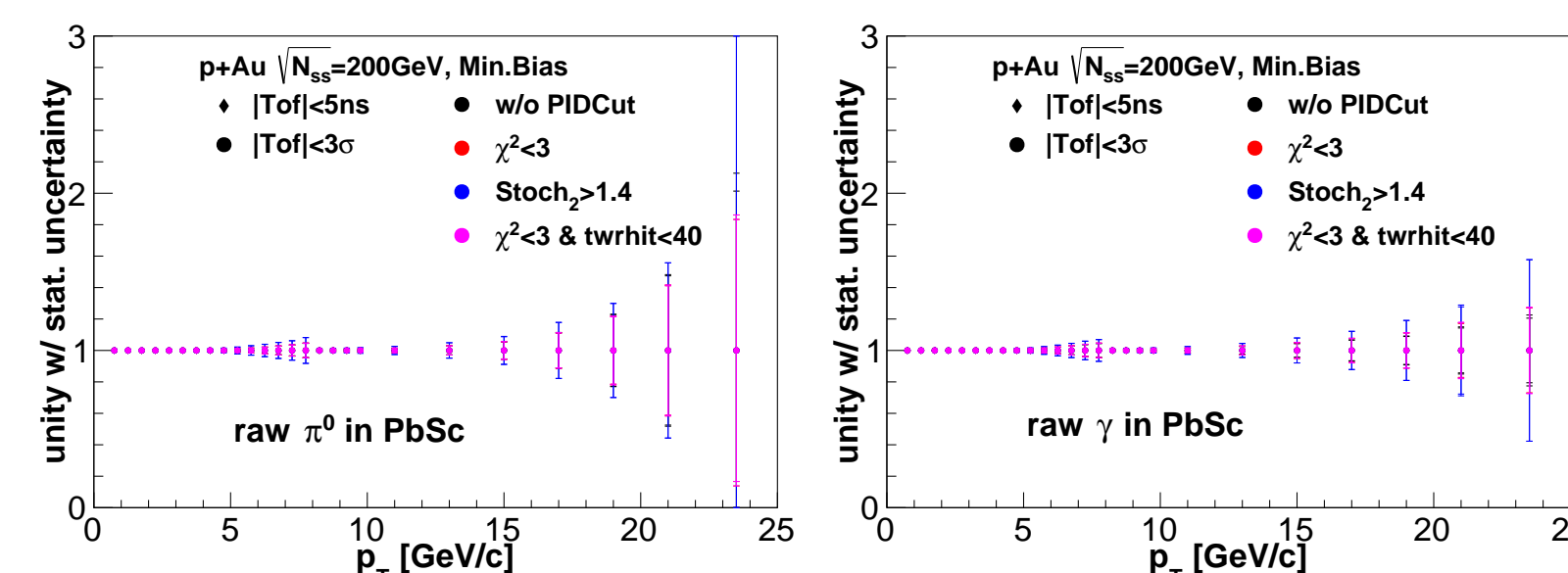


**Figure 2:** The statistical uncertainty in p+Au collisions combining the BBC and ERT triggers for  $\pi^0$  (left panel) and inclusive photons (right panel).

## Timing calibration

Accurate timing information in the EMCal is important for two reasons: it helps to suppress contamination of the photon sample by hadrons, and to eliminate pile-up events. The time-of-flight (ToF) is calculated as

$ToF = -LC(TDC - walk) - t_1^{tower} - t_2^{sec(run)} - t_0^{BBC}$  where  $LC$  is the least count (TDC count to ns conversion factor),  $TDC$  is the raw TDC count,  $walk$  is the energy-dependent walk (slewing),  $t_1^{tower}$  is a fixed offset while  $t_2^{sec(run)}$  is a run-dependent correction for all towers in a sector.  $t_0^{BBC}$  is the zero time of the Beam-beam counter (BBC). After all corrections, TOF is shifted to 0 for photons in order to simplify the analysis.

The widths per sector of the ToF distributions before and after calibration are tabulated in Table 1 and a typical distribution is shown in Fig. 3.

$\sigma$ of ToF (ns), BBC			
Sector	p+p Before	p+p After	p+Au After
0	0.56	0.455	0.445
1	0.56	0.453	0.451
2	0.60	0.487	0.491
3	0.71	0.549	0.600
4	0.72	0.447	0.434
5	0.54	0.501	0.555
6	1.20	0.746	0.665
7	1.44	0.777	0.745

**Table 1:** The  $\sigma$  of ToF before and after calibration in BBC trigger.

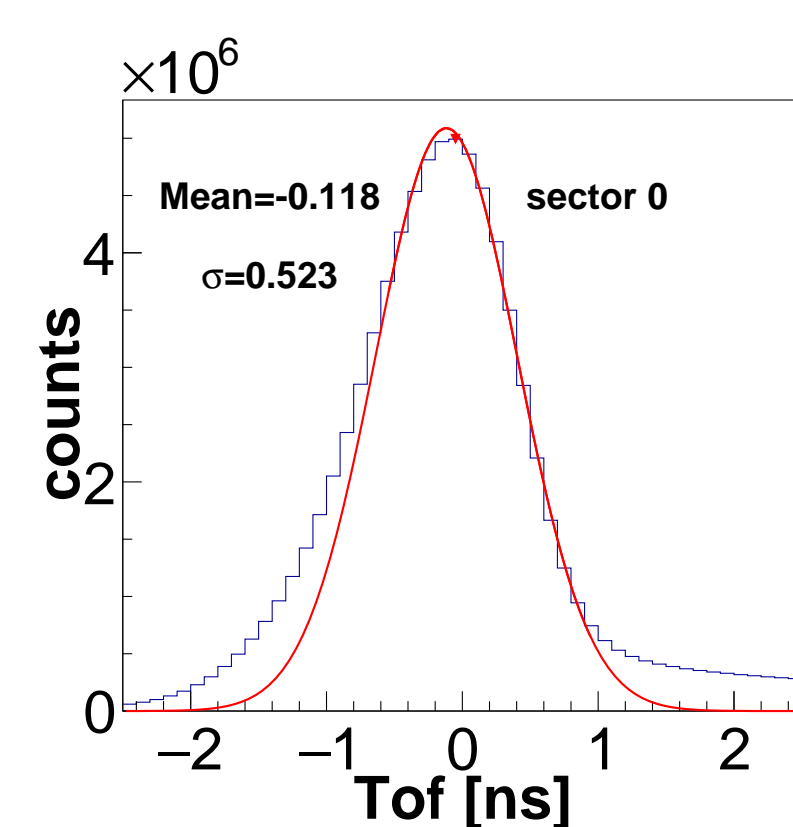


**Figure 3:** The distribution of ToF for sector 0 in p+p (BBC).

## Analysis cuts

**Particle IDentification (PID)** Photons are identified using two different methods. The first compares the observed shower

shape (energy deposit pattern) to the predicted pattern from an electromagnetic shower [3].

$$\chi^2 = \sum_i \frac{(E_i^{meas} - E_i^{pred})^2}{\sigma_i^2},$$

and only accepts showers with  $\chi^2 < 3$ . The second combines different shower characteristics into a single, likelihood-type expression ("stochastic cut"). The two cuts have very different efficiencies, but after proper correction both methods should give the same result.

**Pile-up events, time of flight.** Overlapping events should be discarded from the data sample. In Fig.4 the timing distributions of photon pairs with invariant mass corresponding to a  $\pi^0$  are shown, along with their fraction in the total sample. Photons from pile-up events are eliminated either by a universal  $|tof| < 5.0 ns$  cut or a  $\sigma$ -dependent cut.

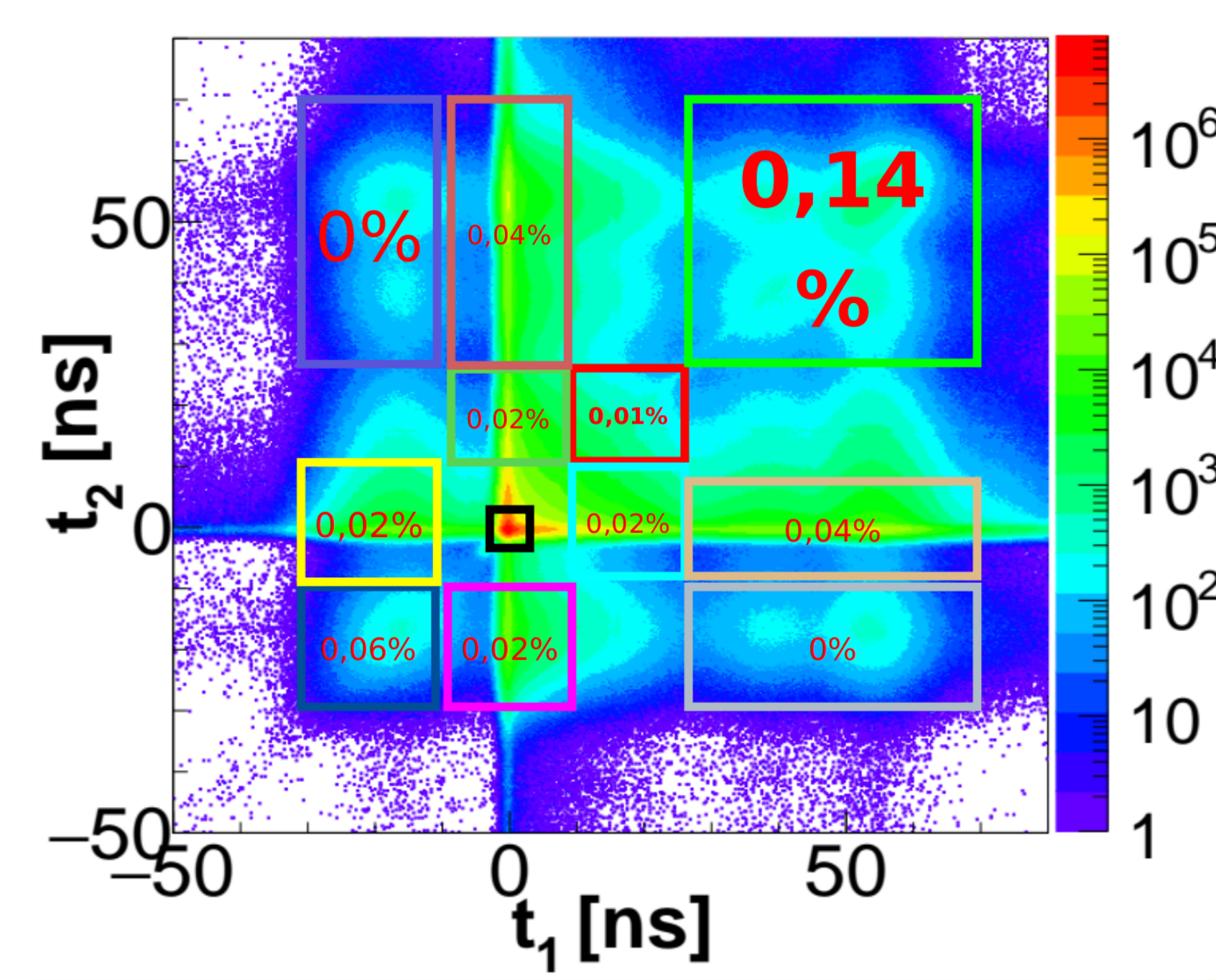


**Figure 4:** 2D distribution of the ToF of  $\pi^0$  candidates. The percentage in each box shows the percentage of  $\pi^0$ 's in each box compared to the black box of  $|tof| < 5 ns$  for both clusters

## Raw $\pi^0$ yield extraction

Photons from  $\pi^0$  decay are the single largest background to the direct photon measurement [4], so it is prudent to analyze them in tandem with inclusive/direct photons, using their  $2\gamma$  decay channel. In Fig. 5 the invariant mass distribution is shown at a given  $p_T$  for real and mixed events as well as after subtraction. Fig. 6 shows the raw  $\pi^0$  invariant yields from the entire (minimum bias and triggered) dataset.

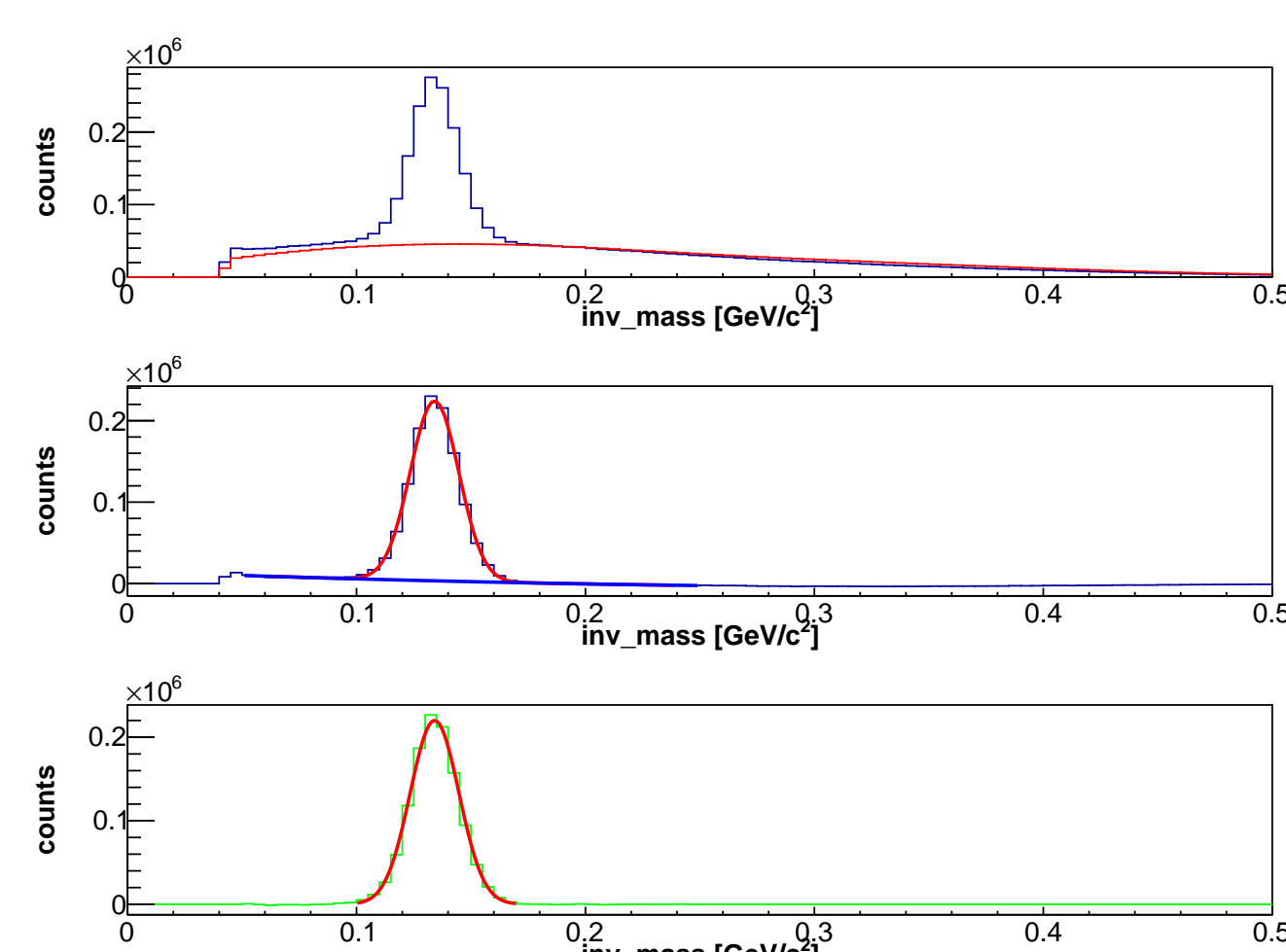


**Figure 5:** Invariant mass of real (blue) and scaled mixed (red) events (top). Linear fit of the residual background (middle). The net  $\pi^0$  peak (bottom).

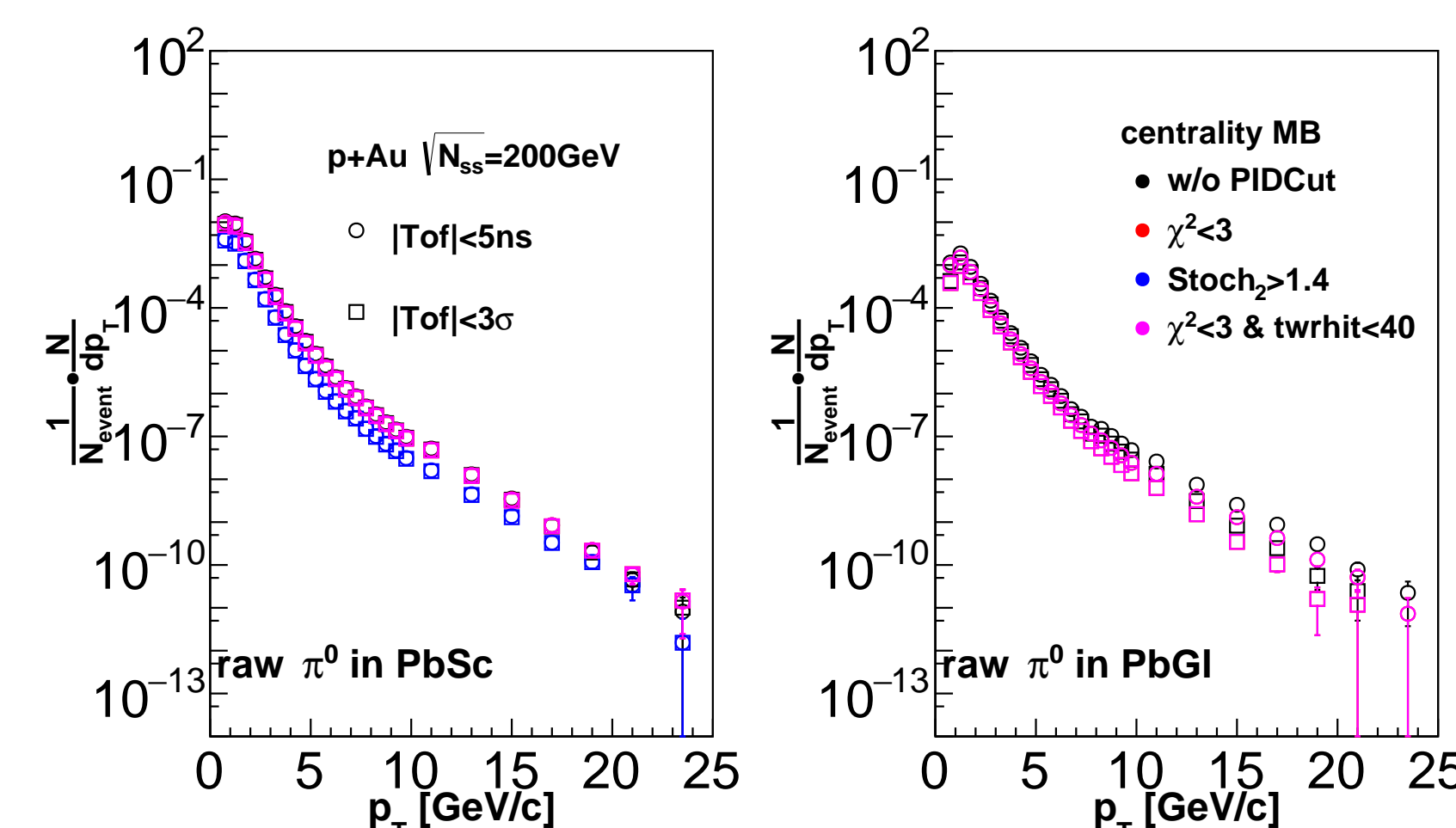


**Figure 6:** The combined spectra of raw  $\pi^0$ , p+Au.

## Raw inclusive photon yields

The raw spectra of inclusive  $\gamma$  yields are obtained with the same photon timing and PID cuts as used in the  $\pi^0$  analysis. The raw yields for the combined BBC and ERT triggers and various cuts are shown in Fig.7.

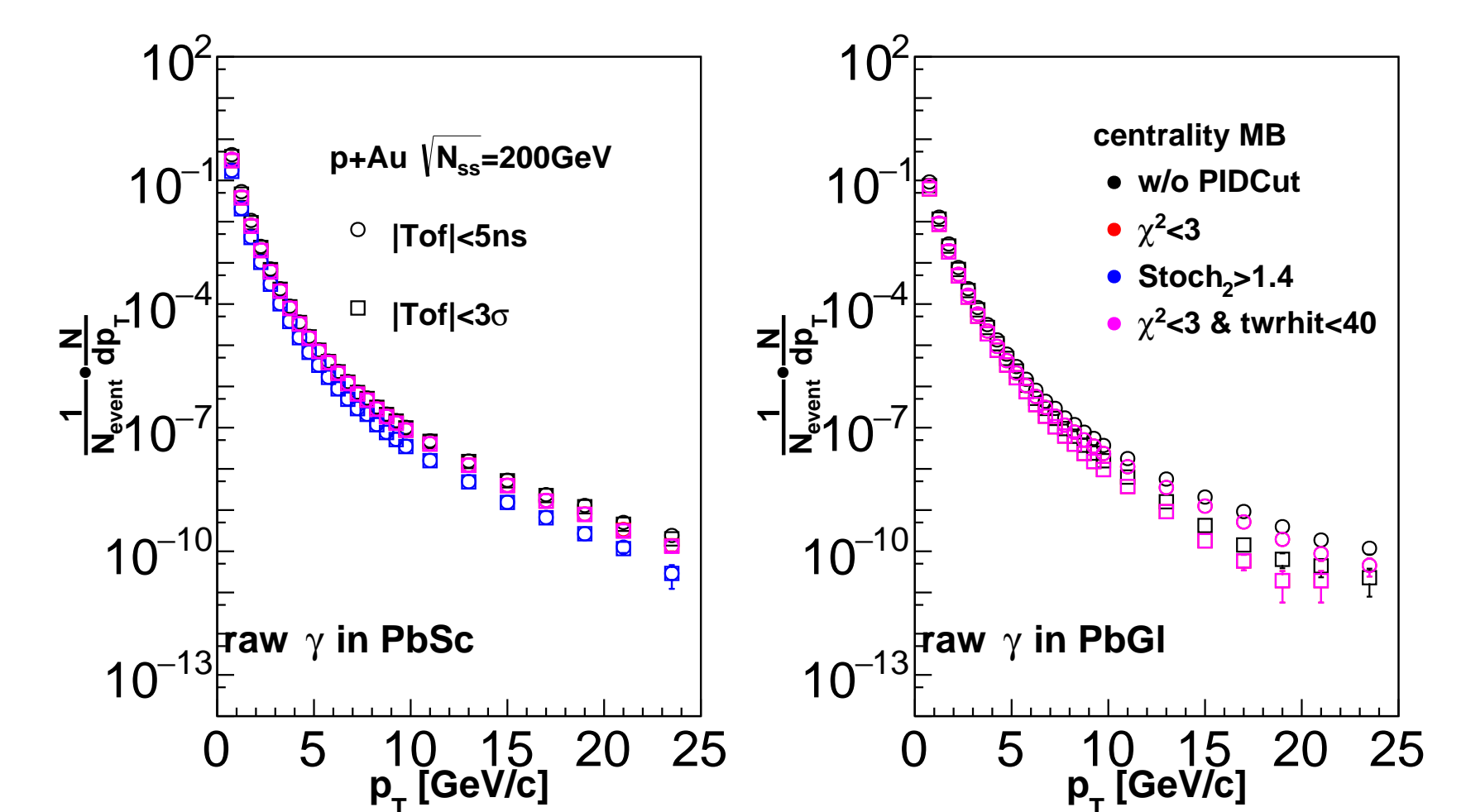


**Figure 7:** The combined spectra of raw  $\gamma$ , p+Au.

## Raw inclusive $\gamma/\pi^0$

According to Sternheimer's formula if all photons come from  $\pi^0$  decay then asymptotically

$$R_{\gamma/\pi^0} = \frac{dN_{\gamma}/dE_{\gamma}}{dN_{\pi^0}/dp_{T\pi^0}} = \frac{2}{n}$$

where  $n$  is the power in the power law distribution of the  $\pi^0$   $p_T$  spectrum ( $f(p_T) = Ap_T^n$ ). Note, however, that the efficiency to measure  $\pi^0$  rapidly decreases with increasing  $p_T$  (merging of photon showers), as shown in Fig 8, so the raw inclusive  $\gamma/\pi^0$  ratio would rapidly increase even in absence of any high  $p_T$  direct photon sources.

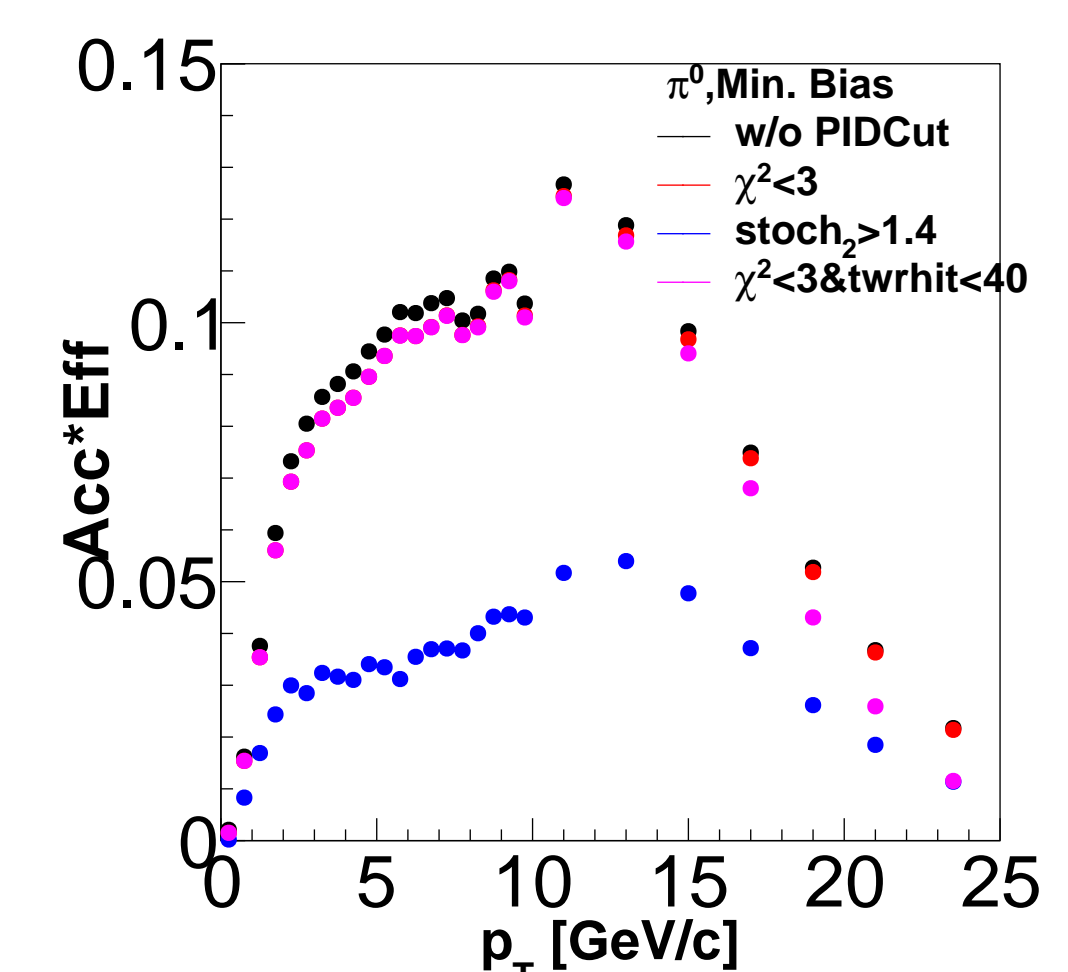


**Figure 8:** The acceptance and efficiency for  $\pi^0$  in MB collisions.

With these caveats the ratios of the raw inclusive photon and  $\pi^0$  spectra are shown in Fig. 9 for p+p and p+Au collisions. The fact that the raw  $\gamma/\pi^0$  ratio is flat at moderate  $p_T$  indicates the sanity of the analysis so far. Since at this point all corrections are missing, there are no physics conclusions to be drawn; the point is that the quality of data is quite good at least up to 17 GeV/c, significantly surpassing earlier (dAu) data, and once the analysis is finished, we will be able to pinpoint for instance the isospin-effect (see Fig. 1).

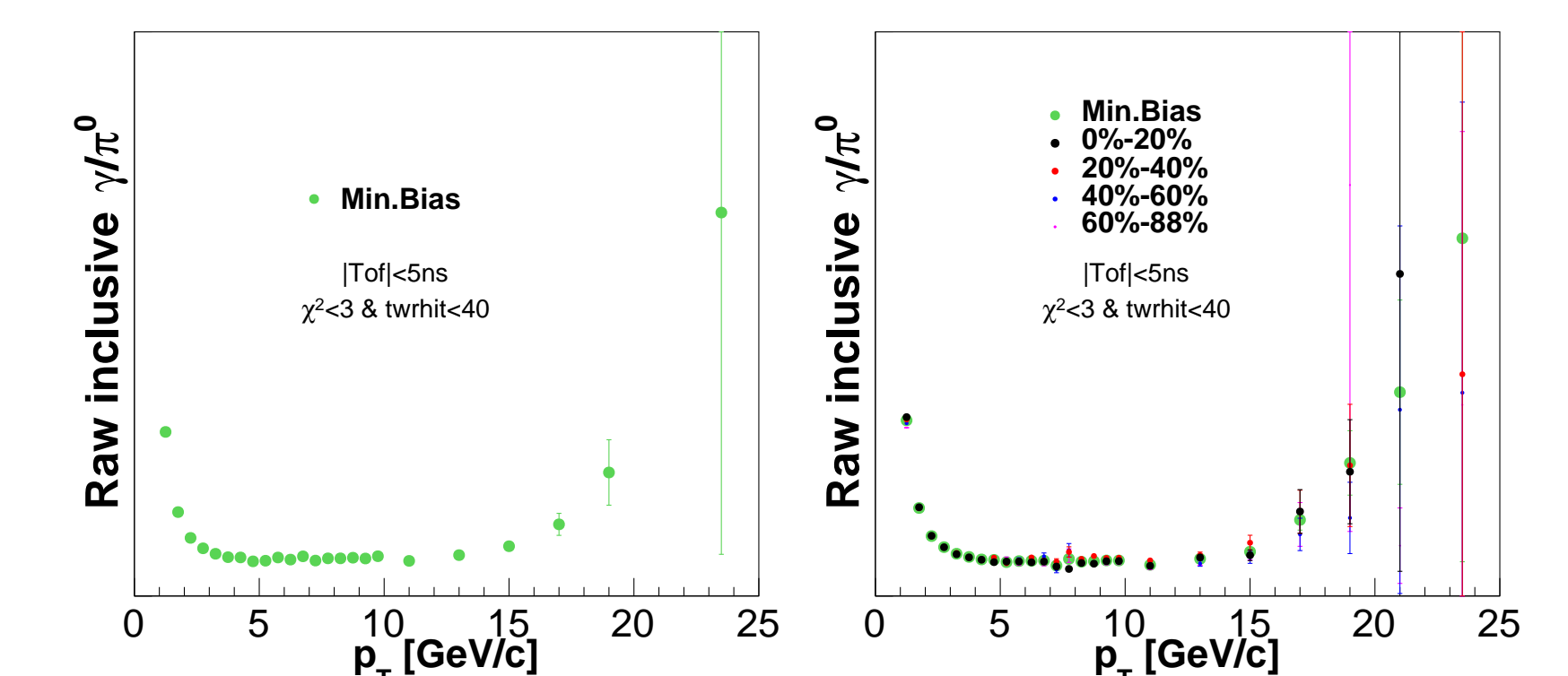


**Figure 9:** Raw  $\gamma/\pi^0$  in p+p (left panel) and p+Au collisions,  $|ToF| < 5 ns$ ,  $\chi^2 < 3$  and towerhit < 40 in centrality bins.

## Conclusions

We reported on the status of the analysis of high  $p_T$  direct photons - along a re-analysis of neutral pions - in p+p and p+Au collisions at RHIC. The timing calibration has been improved and the PID cuts tightened, because inclusive photons are more sensitive to detector effects than  $\pi^0$ 's. So far only raw yields are available, the necessary corrections are work in progress. The irreducible (statistical) uncertainties alone would allow to test the isospin effect as well as the applicability of the Glauber-model up to at least 17 GeV/c.

## References

- [1] Phys. Rev. Lett **109**, 152302 (2012)
- [2] Phys. Rev. C **87**, 054907 (2013)
- [3] A. A. Iedev IHEP preprint 93-153 protvino 1993
- [4] Phys. Rev. C **99**, 024912 (2019)
- [5] NIM A499 521-536 (2003), PHENIX Calorimeter.